ASCE

Time-Dependent Reliability Analysis of Buried Water Distribution Network: Combined Finite-Element and Probabilistic Approach

Weinan Li, S.M.ASCE[1]; Ram K. Mazumder, Ph.D., A.M.ASCE[2]; and Yue Li, Ph.D., M.ASCE[3]

Abstract: Corrosion deterioration is the predominant factor for a large number of cast iron (CI) water main breaks. The reliability of CI pipelines decreases overtime as corrosion growth on pipe walls significantly reduces the strength of pipeline materials. To predict the reliability of water pipelines accurately, this study used a finite-element analysis (FEA) approach to determine the maximum pipeline stress at various stages of the pipeline's life. A series of FEAs was performed to consider uncertainties in parameters associated with stress analysis. The circumferential stress was found to be the most critical stress for pipelines. Time-variant circumferential stress was obtained by accounting for the time-dependent corrosion pit growth on the pipeline wall. The time-variant failure probability of pipelines was determined by comparing the circumferential stress and the tensile failure strength of the pipeline at the burst limit state. The FEA model developed in this study was validated with the results obtained from previous studies. Monte Carlo simulation was performed to generate the fragility curves in a probabilistic manner. This study also compared the fragility curves obtained utilizing FEA and conventional equations (elastic ring theory and the Spangler formula). The results showed that analytical equations are too conservative and provide a higher failure probability of pipeline. A sensitivity analysis was performed to identify the relative importance of parameters contributing to the pipeline's performance. Additionally, the reliability of the water distribution network (WDN) was calculated based on the minimum cut set (MCS) and graph decomposition methods. The results showed that the two methods provide similar outcomes, however, MCS provides a greater safety margin. The proposed approach was illustrated for an example WDN. **DOI: 10.1061/AJRUA6.0001178.** © *2021 American Society of Civil Engineers.*

Introduction

Underground pipeline networks are referred to as essential assets for the public because they transport oil, water, and gas that are vital to human beings. The performance of a pipeline network is very important for the well-being of society. However, statistical data suggest that pipeline failure incidents are experiencing a growing trend, which is expected to affect social wealth and convenience negatively (Mazumder et al. 2018). Aging metallic pipelines are the most vulnerable to failure because a majority of them are in service beyond their expected design life (Folkman 2018). The break rate of water mains is about 14 breaks/161 km (100 mi)/year, and the break rate is increasing continuously. A majority of water pipes in the US are made of cast iron (CI), and pipes laid more than 50 years ago have an increasingly higher break rate (Folkman 2018). To provide a sufficient amount of water to communities, a viable methodology for the maintenance of water pipeline systems is necessary for water utilities. Water pipelines typically are buried underground, and pass beneath roads, railways, and runways. Hence, pipelines should be designed to resist internal pressure, traffic load, soil overburden impact, and other environmental factors.

A significant amount of effort has focused on determining the stress on buried pipelines. Spangler (1941) was among the first to develop a stress determination equation for buried pipelines. Other researchers tried to further improve this equation (e.g., Watkins and Anderson 1999; Masada 2000; Warman et al. 2009). Although these equations have been used widely until recently, there are many unaccounted aspects, including three-dimensional (3D) effects and inconsistent treatment for internal pressure, soil–pipeline interaction, and stress redistribution. To avoid these limitations, researchers analyzed the pipeline's performance by developing finite-element analysis (FEA) models. Robert et al. (2016) developed three-dimensional finite-element models to analyze the stress distribution of buried pipelines subjected to internal pressure and surface traffic loads. They derived a nonlinear regression equation from finite-element analyses to predict pipeline maximum circumferential stress. Zhang et al. (2016) utilized FEA models to investigate the relative importance of various parameters to the performance of pipelines, which is illustrated by the von Mises stress, vertical displacement, and ovality. They determined that pressurized pipelines have less likelihood of failure than do nonpressurized pipelines. They found that the diameter to thickness ratio, buried depth, soil cohesion, and elastic modulus of the pipe are the key factors that influence the performance of pipelines. Neya et al. (2017) modeled buried pipelines under moving traffic loads using FEA, and the results indicated that the maximum principal stress decreases as vehicle velocity increases. Ji et al. (2017) created an equation for predicting the stress concentration factor, defined as the ratio of concentrated stress of corrosion pit to the uniformly

[1]Graduate Research Assistant, Dept. of Civil and Environmental Engineering, Case Western Reserve Univ., Cleveland, OH 44106 (corresponding author). Email: wxl556@case.edu

[2]Postdoctoral Researcher, Dept. of Civil, Environmental and Architectural Engineering, Univ. of Kansas, Lawrence, KS 66045. Email: rkmazumder@ku.edu

[3]Leonard Case Professor in Engineering, Dept. of Civil and Environmental Engineering, Case Western Reserve Univ., Cleveland, OH 44106. Email: yxl1566@case.edu

Note. This manuscript was submitted on December 17, 2020; approved on May 21, 2021; published online on September 7, 2021. Discussion period open until February 7, 2022; separate discussions must be submitted for individual papers. This paper is part of the ***ASCE-ASME Journal of Risk and Uncertainty in Engineering Systems, Part A: Civil Engineering***, © ASCE, ISSN 2376-7642.

corroded pipe stress. They also developed fragility curves and hazard rates based on theoretical equations. However, Ji et al. (2017) did not consider the impacts of other parameters, such as soil elastic modulus, internal pressure, and traffic load, in the fragility curves of the pipelines. Although those studies provide a significant contribution to determining the stress and performance of pipelines, most of the past FEA-based studies did not account for the effect of corrosion on the performance of the pipelines.

Buried pipelines often are exposed to aggressive soil environments. Due to the corrosive effects of the surrounding environment, and buried pipeline strength decreases overtime with corrosion growth on the pipeline's wall. Corrosion is a crucial factor particularly for pipelines that were laid earlier in the last century and are still in use in many municipalities (Ji et al. 2017). The corrosion growth rate depends on many factors, such as the pipeline material properties, type of internal fluid, and surrounding soil corrosivity. The strength of the pipeline decreases gradually with corrosion growth and eventually causes failure if the stress on the pipeline exceeds the tensile strength of the pipeline (Ahammed 1998). In structural reliability analysis of pipelines, the failure probability of a pipeline is estimated by comparing the stress on the pipeline and strength of the pipeline. Time-dependent failure probability can be determined by incorporating the time-variant effect of corrosion on pipeline performance. Two types of corrosion (i.e., uniform and pitting) typically are formed on the pipeline wall. However, because stress concentration occurs on the pipeline at the location of maximum depth of corrosion pit, most time-variant pipe reliability analyses studies consider the pitting corrosion model. Analytical approaches accounted for the effect of corrosion deterioration on pipeline performance. Ahammed (1998) developed a reliability model by comparing pipeline failure pressure and applied internal pressure. Caleyo et al. (2002) compared five failure pressure models and provided several suggestions for the selection of model type according to specific cases. Another simple tool for pipeline safety assessment was presented by Wang and Zarghamee (2014), who conducted a series of reliability analyses of burst pressure and service limit using the FEA models, and derived the best fitting equation for retained strength. The pipeline model was generated with cuts in the pipeline's surface to consider corrosion.

The performance of a water distribution network (WDN) depends not only on the performance of an individual pipeline but also on its network configuration (Deuerlein et al. 2009). Hence, system-level reliability needs to be assessed. The reliability analysis of WDNs can be categorized into two main approaches: (1) mechanical reliability, and (2) hydraulic reliability (Mazumder et al. 2019). Mechanical reliability is estimated using the connectivity approach, in which network reliability requires that all demand nodes have at least one connection to the water source node. On the other hand, hydraulic-based reliability is measured by the amount of water availability at demand nodes (Ostfeld 2004). WDNs in modern society typically are complex and large. Hundreds of pipelines and nodes in a single WDN make the maintenance and control very difficult. Several reliability assessment approaches exist in the literature [e.g., fault trees and minimum cut sets (MCS)] to determine the system reliability of WDNs. Among these approaches, the minimum cut set is a well-defined method in network reliability calculation and is more convenient and efficient than other reliability calculation methods (Tung 1985). The adjacency matrix can be utilized to find the number of MCS of a WDN, as described by Yannopoulos and Spiliotis (2013). The graph decomposition method developed by Deuerlein (2008) also provides a better understanding and identification of complex networks. Deuerlein et al. (2009) introduced a new method combining hydraulic reliability and connectivity-based reliability to calculate the reliability of WDNs.

This study developed several FEA models for accurately estimating the failure pressure on the pipelines. To estimate the pipe stress, the effect of corrosion is accounted for by incorporating the corrosion pit on the pipeline wall. A series of FEA models was developed to obtain the statistical distribution of the circumferential stress to account for uncertainties in parameters. The predicted coefficient of variance and distribution type of the circumferential stress was utilized for modeling probabilistic failure analysis of pipelines at the burst limit state. Fragility curves were developed utilizing the stress obtained from both FEA and analytical models. Additionally, this study performed a sensitivity analysis to identify the relative importance of parameters contributing to the pipeline's performance. The system-level performance of WDS was estimated utilizing the MCS method and the graph decomposition method. The proposed approach was illustrated for a simple network. This study focused on large-diameter pipelines because the failure of large-diameter pipelines incurs significant financial losses and environmental impacts.

Methodology

In this study, finite-analysis models were developed to determine the stress on the pipeline. A three-dimensional FEA model was developed using Abaqus version 2016. To account for the uncertainty associated with parameters involved in stress calculation, a large number of FEA models were developed. Results obtained from FEA were fitted to a statistical model to determine the randomness of stresses. A time-dependent corrosion pit on the pipeline wall was incorporated to obtain the time-dependent stress on the pipeline. Pipeline failure at the burst limit state was evaluated by comparing the stress on the pipeline and the tensile strength of the pipeline. Fragility curves for burst failure of pipelines were developed using Monte Carlo simulation. The burst failure probability of the pipelines was determined using fragility curves. Because the performance of the water network does not depend only on a single pipeline, system reliability was estimated for the network utilizing MCS and graph decomposition methods. A sensitivity analysis was performed to compare the importance of various parameters to the pipeline performance. Fig. 1 shows the workflow chart of this study.

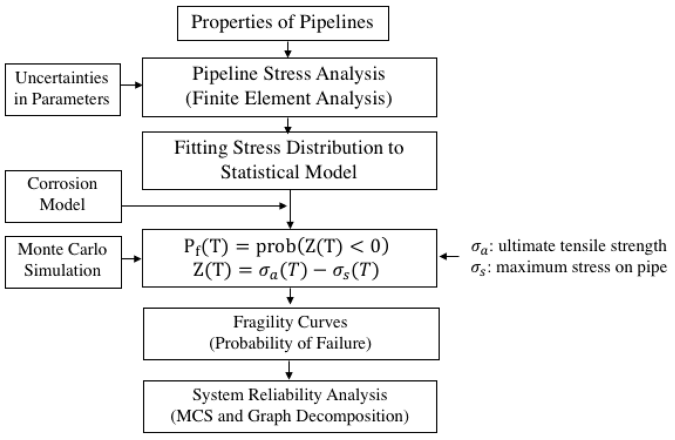

Fig. 1. Flow chart of proposed methodology.

Pipeline Stress Analysis: Analytical Approaches

Because buried water pipelines typically are subjected to live traffic loads, soil-cover dead loads, and internal water pressure, most analytical stress estimation equations were developed considering these factors. Large traffic loads, such as truck loads, railway loads, and locomotive loads, are particularly noteworthy because they impose impact loads on pipelines. The pipeline maximum stress under external loads can be calculated using the elastic ring theory proposed by Watkins and Anderson (1999)

$$\sigma = \frac{1.5qD^2}{4t^2} \tag{1}$$

where q = uniform vertical load due to traffic and soil loads; D = pipeline diameter; and t = pipeline thickness. The concentrated traffic load transmitted to buried pipelines can be calculated by Boussinesq's equation (Moser and Folkman 2008)

$$\rho_p = \frac{3F_s}{2\pi C^2[1+(\frac{d}{C})^2]^{2.5}} \tag{2}$$

where ρ_p = pressure transmitted to pipeline; F_s = concentrated traffic load at surface; C = depth of soil cover; and d = distance from pipeline to line of applied surface traffic load.

Spangler (1941) formulated the stress equation for a pipeline's maximum circumferential stress subjected to vertical loads. Moreover, Spangler (1941) combined elastic ring theory and three unique full-load hypotheses to create the original Iowa formula to calculate a pipeline's horizontal deflection. Masada (2000) modified the Iowa formula to calculate a pipeline's vertical deflection. One of the main advantages of the Spangler formula is that it considers the supports received from the pipeline's surrounding soil. A uniformly distributed pressure at the bottom of the pipeline is assumed in the Spangler formula, and bedding angle is a factor impacting soil supporting pressure. Moreover, it is assumed that horizontal pressure on each side of the pipeline is proportional to pipeline horizontal deflection. The pipeline horizontal deflection and maximum stress in the Spangler formula and modified Iowa formula are, respectively

$$\Delta X = \frac{L_\Delta K W_{\text{vertical}} r^3}{EI + 0.061E'r^4} \tag{3}$$

$$\sigma = \frac{6K_b W_{\text{vertical}} Etr}{Et^3 + 24K_Z\rho r^3 + 0.732E'r^3} \tag{4}$$

where ΔX = horizontal defection of pipe; L_Δ = deflection lag factor; K = bending constant; W_{vertical} = vertical load due to soil cover and traffic load; r = radius of pipe; E = elastic modulus of pipe material; I = moment of inertia of pipe section; E' = modulus of passive soil resistance; ρ = internal pressure; K_b = bending moment parameter; and K_Z = deflection parameter.

Ji et al. (2017) used Robert et al.'s (2016) stress prediction equation to develop fragility curves of buried pipelines

$$\sigma = \frac{W+\gamma D^2 h}{D^2}\cdot\alpha_1\left(\frac{E}{E'}\right)^{\beta_1}\left(\frac{E'}{\gamma h}\right)^{\beta_2} \times\left[\alpha_2\frac{(\frac{\rho}{E'})^{\beta_3}}{(\frac{t}{D})^{\beta_4}\left(\frac{W}{\gamma D^2 h}+1\right)^{\beta_5}} + \alpha_3\frac{(\frac{t}{D})^{\beta_6}\left(\frac{W}{\gamma D^2 h}+1\right)^{\beta_7}}{\alpha_4(\frac{E_\rho}{E'})+\alpha_5(\frac{\rho}{E'})+\alpha_6(\frac{h}{D})+\alpha_7\kappa}\right] \tag{5}$$

where σ = maximum stress on pipe; W = traffic loads; h = buried depth; κ = model uncertainty coefficient; and α and β = model coefficients. The model coefficients α and β ($\alpha_1 = 0.12$, $\alpha_2 = 4.08$, $\alpha_3 = 1.76\times10^6$, $\alpha_4 = 7.65\times10^4$, $\alpha_5 = 4.17\times10^6$, $\alpha_6 = -3.23\times10^7$, $\alpha_7 = -3.55\times10^7$, $\beta_1 = 0.086$, $\beta_2 = 0.94$, $\beta_3 = 0.89$, $\beta_4 = 0.88$, $\beta_5 = 0.94$, $\beta_6 = -0.51$, and $\beta_7 = -0.71$) were taken from Robert et al. (2016).

Corrosion Model

Several corrosion models for metallic pipelines were documented in past research (e.g., Kucera and Mattson 1987; Rajani and Maker 2000; Caleyo et al. 2009; Petersen and Melchers 2012). Mechanisms of corrosion depend on many factors such as pipeline material, environment, and soil conditions. Two types of corrosion are formed on metallic pipeline walls: (1) pitting, and (2) uniform corrosion. Uniform corrosion is an all-around thickness reduction, and pitting corrosion is a localized form of corrosion that may cause holes and cavities (Ji et al. 2017). Pitting corrosion is considered more dangerous than uniform corrosion because it can lead to failure with relatively less loss of pipeline thickness (Ji et al. 2017). For a corrosion cluster with two or more adjacent corrosion defects, the cluster depth is the deepest defect depth of all adjacent defects, and the cluster length is the overall length of adjacent defects in the longitudinal direction. Of the existing models, the corrosion model provided by Petersen and Melchers (2012) was used in this study to model the corrosion pit on the CI pipeline wall. This model was selected because it originally was developed based on field data of corrosion pits on cast iron pipes in various soil conditions. This model has a bilinear trend of corrosion growth in which the corrosion rate high is initially, and then decreases quickly before reaching a steady state. The corrosion models provide the depth of corrosion pits, $\tau(T)$, over time, as provided by Petersen and Melchers (2012)

$$\tau(T) = \begin{cases} \left(\frac{c_s}{T_1}+\delta_s\right)\times T, & \text{when } T < T_1 \\ c_s + \delta_s \times T, & \text{when } T \geq T_1 \end{cases} \tag{6}$$

where c_s = intercept; δ_s = corrosion rate at steady state; T = exposure time; and T_1 = point at which corrosion growth rate reaches steady state.

Finite-Element Analysis

FEA is used numerically to model complex structures, various loading cases, surface conditions, and material properties. Fig. 2 shows a 3D finite-element model of the water pipeline developed in this study. Only pitting corrosion was modeled in the FEA to account for the effect of corrosion on pipeline performance. The initial corrosion depth and length were assumed to be zero. The depth of the corrosion pit was measured using Eq. (6), and the length of the pitting surface was 5 times the depth of the corrosion pit (Petersen and Melchers 2014; Cerit et al. 2009; Wang et al. 2017). The corrosion pit was assumed to be located on the top of the pipeline. Because the pipeline and surrounding soil were symmetric with respect to the y, z-plane, half-models were generated in the FEA to reduce the computational effort. Additionally, the half-model was usable because its results had good agreement with the full-scale model. The pipeline was modeled as a 3D shell instance, whereas the surrounding soil was modeled as a three-dimensional extrusion instance. A meshing size of 0.1 mm was applied to the pipeline instance, and the

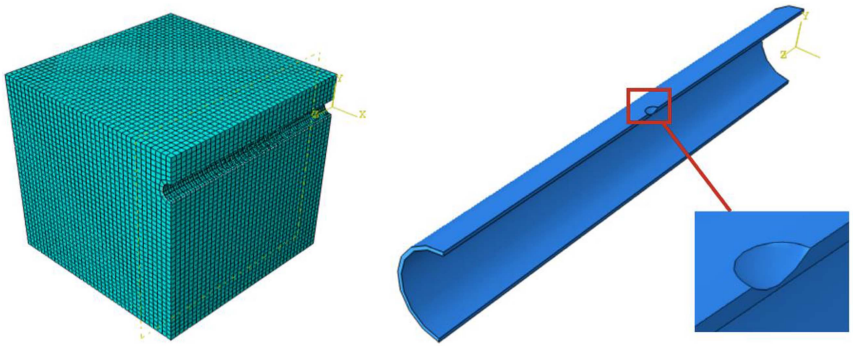

Fig. 2. FEA model: (a) pipeline with surrounding soil; and (b) corrosion defect on pipeline wall.

element type of the pipeline was S4R (a four-node doubly curved thick shell element with reduced integration). The meshing size for the surrounding soil was 0.2 m, and the element type of the soil was C3D8R (an eight-node linear brick element with reduced integration). Robert et al. (2016) showed that there is a negligible influence on pipeline stresses from perfectly elastic or elastoplastic surrounding soil. Therefore, a linear elastic soil model was applied for convenience. The friction coefficient between the soil and the pipeline was 0.3 for the surface contact property. The selection of boundary conditions is extremely important in finite-element analysis, even at a dominant level. To obtain more-accurate results, boundary conditions need to be adjusted so that FEA results can match lab test results. The bottom soil surface was fixed in terms of vertical movement, and four lateral soil faces were fixed in out-of-plane displacements. Because the pipeline model had symmetrical characteristics with respect to the y, z-plane, two pipeline longitudinal cutting faces were assigned symmetrical to the x-axis. The surface traffic load was treated as a concentrated load, acting directly over the middle of the pipeline. The gravity load was added with gravitational acceleration of 9.81 m/s^2. Table 1 lists the basic physical properties of the model.

The stresses and strains were defined on the basis of uniaxial cases; however, there are limited uniaxial cases in real life. In this model, the pipeline has mixtures of stresses and strains in various directions. Because the stress–strain relationship of pipeline material is accessible only in the uniaxial case, complicated stresses and strains must be transformed into a uniaxial case. The von Mises stress is an effective tool to relate actual stresses to equivalent uniaxial stress (Ling 1996)

$$\sigma_e = \frac{1}{\sqrt{2}}\sqrt{(\sigma_x-\sigma_y)^2+(\sigma_y-\sigma_z)^2+(\sigma_x-\sigma_z)^2+6(\tau_{xy}^2+\tau_{yz}^2+\tau_{xz}^2)} \tag{7}$$

where σ_x, σ_y, and σ_z = normal stress in x-, y-, and z-directions, respectively; and τ = shear stress.

Table 1. Physical properties of pipeline model in FEA

Parameter	Value
Pipeline diameter (mm)	600
Pipeline thickness (mm)	25
Pipeline length (m)	7.5
Buried depth (m)	0.8
Surface traffic load (kN)	70
Internal pressure (kPa)	1,000
Pipeline elastic modulus (GPa)	100
Soil elastic modulus (MPa)	25
Tensile strength (MPa)	100

FEA Model Validation

FEA models were calibrated by comparing FEA results with experimental test results. To validate a newly generated model, results from the FEA model were compared with field test results and results of Robert et al.'s (2016) FEA model. Robert et al. (2016) validated the FEA model using field test data; the traffic load was a single-axle single-tire truck with an axle load of 4,850 kg (4.85 t). The circumferential stresses were measured for three cases. The truck was not moving in the first case (Fig. 3, Field stopping), and it was moving at 5 and 15 km/h in the second and third cases, respectively. The model generated in this study used the same geometries and loading conditions as Robert et al. (2016) to validate the model. The magnitude of the truck load applied to the present FEA model was reduced by 50% because the half-scale pipeline section was modeled. The diameter, thickness, and length of the pipeline were 660 mm, 25 mm, and 7.5 m, respectively. The density and elastic modulus of the pipeline were 7,850 kg/m^3 and 210 GPa, respectively. The plastic strain of pipeline material was

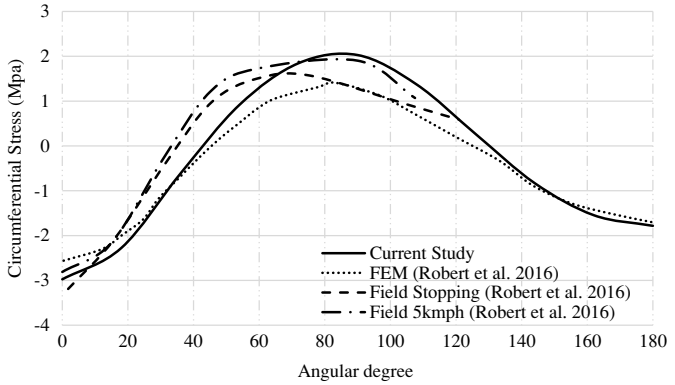

Fig. 3. Comparison of circumferential stress between present FEA model and literature.

equal to zero before reaching the yield stress, which was 450 MPa, and then it increased to 0.06 when stress reached 600 MPa. Fig. 3 compares pipeline circumferential stress distribution curves developed utilizing various models. The present model accurately predicted the pipeline circumferential stress distribution. For example, the maximum stress from Robert et al.'s (2016) FEA model was 25.5 MPa, whereas the maximum stress obtained in the present study was 27.34 MPa. An internal pressure of 900 kPa was used in the FEA model. The results of the present study slightly differed from the results obtained by Robert et al. (2016). The difference may be attributed to different meshing sizes, element assumptions, and external loading patterns. It can be concluded that the present FEA model is validated and usable for further study.

Pipeline Reliability Analysis: Burst Failure Limit

Pipeline maximum stress varies with the variation of pipeline geometries and material properties. Reliability analysis is a practical method to analyze the failure probability of the pipeline because it is able to consider these uncertainties (Mazumder et al. 2019). Burst failure of a pipeline is defined as the condition in which maximum stress on the pipeline exceeds the pipeline's stress capacity. First, a burst limit state function, providing failure criteria, needs to be defined in probability analysis method. The circumferential stress was used in the limit state function because circumferential stress was the most critical stress observed in this study. The limit state function is

$$Z(T) = \sigma_a(T) - \sigma_s(T) \tag{8}$$

where σ_a = pipeline stress resistance; and σ_s = pipeline maximum stress due to applied loads. The pipeline is said to be failed when $Z < 0$. Therefore, the failure probability of the pipeline is

$$P_f(T) = \text{Prob}[Z(T) < 0] \tag{9}$$

Monte Carlo simulation was used to analyze the failure probability of the pipeline; N is the number of simulations carried out during each instant; and n is the number of failure states (i.e., $Z < 0$). Therefore, the failure probability of a pipeline is calculated as follows:

$$P_f = n/N \tag{10}$$

The pipeline reliability is the complement of pipeline failure probability (P_f), and it is expressed as the follows:

$$R = 1 - P_f \tag{11}$$

The fragility curves provide the time-dependent failure probability of buried water pipes, and thus provide useful information for pipeline maintenance decisions.

The distribution type and coefficient of variance of pipeline circumferential stress due to parameter variations need to be investigated to conduct reliability analysis. Pipeline circumferential stresses were obtained under small variations of five factors, namely pipeline diameter, pipeline thickness, pipeline elastic modulus, buried depth, and internal pressure. As suggested by Ahammed (1998) and Wang and Zarghamee (2014), the elastic modulus was considered to be lognormally distributed, and the rest of the parameters were normally distributed. Table 2 lists the statistical distribution of these parameters. Limited efforts have investigated the correlations among the parameters on the performance of buried oil and gas pipelines, including studies by De Leon and Macías (2005), Qian et al. (2013a, b), and Zhang et al. (2019). However, studies investigating the effect of parameters' correlation on performance of water pipeline is rare. The stress prediction equation used in this study ignored the influence of the correlation between parameters on pipeline performance.

Table 2. Statistical distributions of random variables

Parameter	Mean	COV	Distribution type
Pipeline diameter (mm)	600	0.03	Normal
Pipeline thickness (mm)	25	0.05	Normal
Pipeline elastic modulus (GPa)	100	0.08	Log-normal
Buried depth (m)	0.8	0.05	Normal
Internal pressure (kPa)	1,000	0.1	Normal

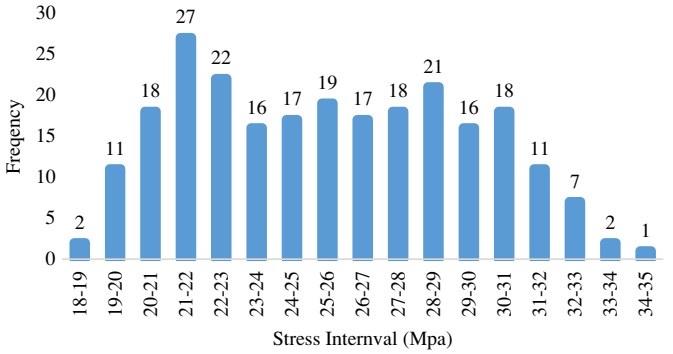

Fig. 4. Circumferential stress distribution.

In the initial state, 243 models were developed for FEA to determine stress distribution patterns. The average required time for a simulation was 30 min on a personal computer with a 2.10-GHz Intel Core i5 processor with 8 GB RAM. The stress distribution obtained from the FEA analyses is shown in Fig. 4. The stress distribution was fitted for four distribution types: normal, lognormal, Gumbel, and Weibull distributions. The Kolmogorov–Smirnov goodness-of-fit test was performed to determine the best-fitted distribution (Ang and Tang 2007). The maximum differences D_{243} obtained were 0.0838, 0.0939, 0.0991, and 0.0967 for normal, lognormal, Gumbel, and Weibull distributions, respectively. The critical value was 0.0872 at a 5% significance level. The normal distribution was found to give the best fit for the stress distribution. Therefore, the pipeline circumferential stress distribution was assumed to be a normal distribution with a coefficient of variation of 0.15 for estimating the fragility curves of the pipelines.

Fragility Analysis

The failure probability of the pipeline was determined by comparing the circumferential stress and the tensile strength of the pipeline's material using Monte Carlo simulation. The pipeline geometries and properties are provided in Table 1. Fragility curves were developed for a large-diameter pipeline (600 mm diameter, 25 mm thick, 100 GPa elastic modulus, and 0.8 m buried depth). The pipeline was subjected to 1.0 MPa internal pressure and 70 kN surface traffic load. The growth rate of corrosion was 0.12 mm/year based on an observed corrosion data set of aging cast iron pipelines investigated by Petersen and Melchers (2014). To obtain the maximum pipeline stress at various stages of the pipeline's life, von Mises stress, circumferential stress, and radial stress were recorded with exposure time. Fig. 5 shows increasing trends of the three types of stresses overtimes. The von Mises stresses and

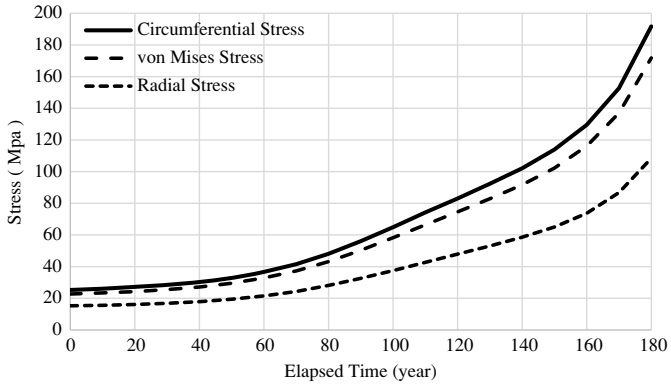

Fig. 5. Time-variant stresses on pipeline.

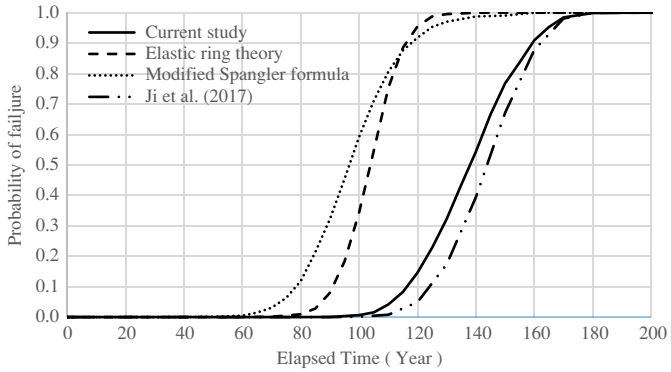

Fig. 6. Time-dependent failure probability curves of pipelines.

circumferential stresses had similar values because their differences were within 10%; however, radial stresses had much lower values in comparison. Circumferential stresses were the highest among the three types of stresses; therefore, the maximum pipeline stresses were represented by circumferential stress.

To generate fragility curves and time-dependent failure probabilities using the limit state [Eq. (8)], time-dependent stress obtained from Fig. 5 was incorporated in the limit state equation, and a coefficient of variation (COV) of 0.15 was used to account for uncertainties involved in stress estimation. Monte Carlo simulation was performed to obtain the burst failure probability of pipelines using the statistical distribution provided in Table 2. The time-dependent failure probabilities of pipelines based on the FEA results are shown in Fig. 6. The present approach provided a failure probability of the pipeline of nearly zero to 100 years, and the failure probability increased exponentially after 100 years (Fig. 6). This study also estimated the fragility curves in which the maximum stresses were calculated based on two theoretical equations with the same corrosion rate of 0.12 mm/year: (1) elastic ring theory [Eq. (1)], and (2) the modified Spangler formula [Eq. (4)]. Table 3 compares the pipeline's maximum stress derived from elastic ring theory and the modified Spangler formula with the FEA results. The theoretical equations provided higher maximum stresses, and stress derived from elastic ring theory increased rapidly with time. The stress overprediction of theoretical equations could be due to the lack of lateral soil support and ignoring the stress redistribution of the pipeline. Time-dependent failure probabilities obtained using various approaches are presented in Fig. 6.

Table 3. Maximum stresses using present FEA and theoretical equations (MPa)

Years elapsed	Stress		
	Present FEA results	Elastic ring theory	Modified Spangler formula
80	48.11	66.41	81.64
90	56.08	78.11	92.19
100	64.92	93.19	104.17
110	74.22	113.11	117.42
120	83.05	140.17	131.40
130	92.39	178.25	144.93
140	102.11	234.26	155.87

Time-dependent failure probability curves obtained using elastic ring theory and the modified Spangler formula varied significantly and were too conservative compared with the curves developed using Ji et al.'s (2017) approach and the present approach. The time-dependent failure probability curves developed using Ji et al.'s (2017) approach and the present approach had similar trends because both of these curves were generated using the same properties of the pipelines. Hence, the present approach is validated by the curve obtained from Ji et al. (2017).

Sensitivity Analysis

Parameters influencing the performance of buried water pipelines may have different contributions to the pipe performance. Sensitivity analysis was performed to investigate the relative contribution of parameters associated to pipeline performance. Five parameters (i.e., pipe thickness, pipe elastic modulus, surrounding soil modulus, internal pressure, and surface traffic load) were selected for sensitivity analysis. To perform sensitivity analysis of each parameter, the investigated parameters were varied from −80% to +120% of the initial value in Table 1 while other parameters were kept at the default values. Fig. 7 shows the effects of each parameter on the failure probability of pipelines. The internal pressure, traffic load, and pipeline elastic modulus had positive effects on the failure probability, indicating that pipeline failure probability increases as these parameters' values increase, and vice versa. The other two parameters, thickness and soil elastic modulus, had negative effects on the failure probability. Additionally, thickness was the predominant parameter because thickness variation had most significant impact on the fragility curve, followed by internal pressure and traffic load. For example, at 120 years, the failure probability was almost 100% for 20-mm-thick pipe, and it decreased to 15% and 0% for pipe with a thickness of 25 and 30 mm, respectively. Hence, it can be said that the most effective way to enhance pipe reliability and service time is to use thicker pipelines in the design state. In terms of applied loads, internal pressure had more impact than surface ground load. Pipeline elastic modulus and soil elastic modulus had limited effects on probability of failure. Generally, the pipeline's elastic modulus was determined by material's yield stress. Although this study suggests that a pipeline's elastic modulus has a limited effect on the failure probability, the selection of the pipe material has a significant influence on the failure probability. Therefore, the use of higher-grade material for pipeline will definitely help to reduce the failure probability. The internal pressure was assumed to be constant (1,000 kPa) when developing these fragility curves (Mazumder et al. 2019).

Fig. 8 shows how the probability of failure changes with the change of internal pressure at various ages of pipeline. In this case, the failure probabilities increased more quickly as the internal

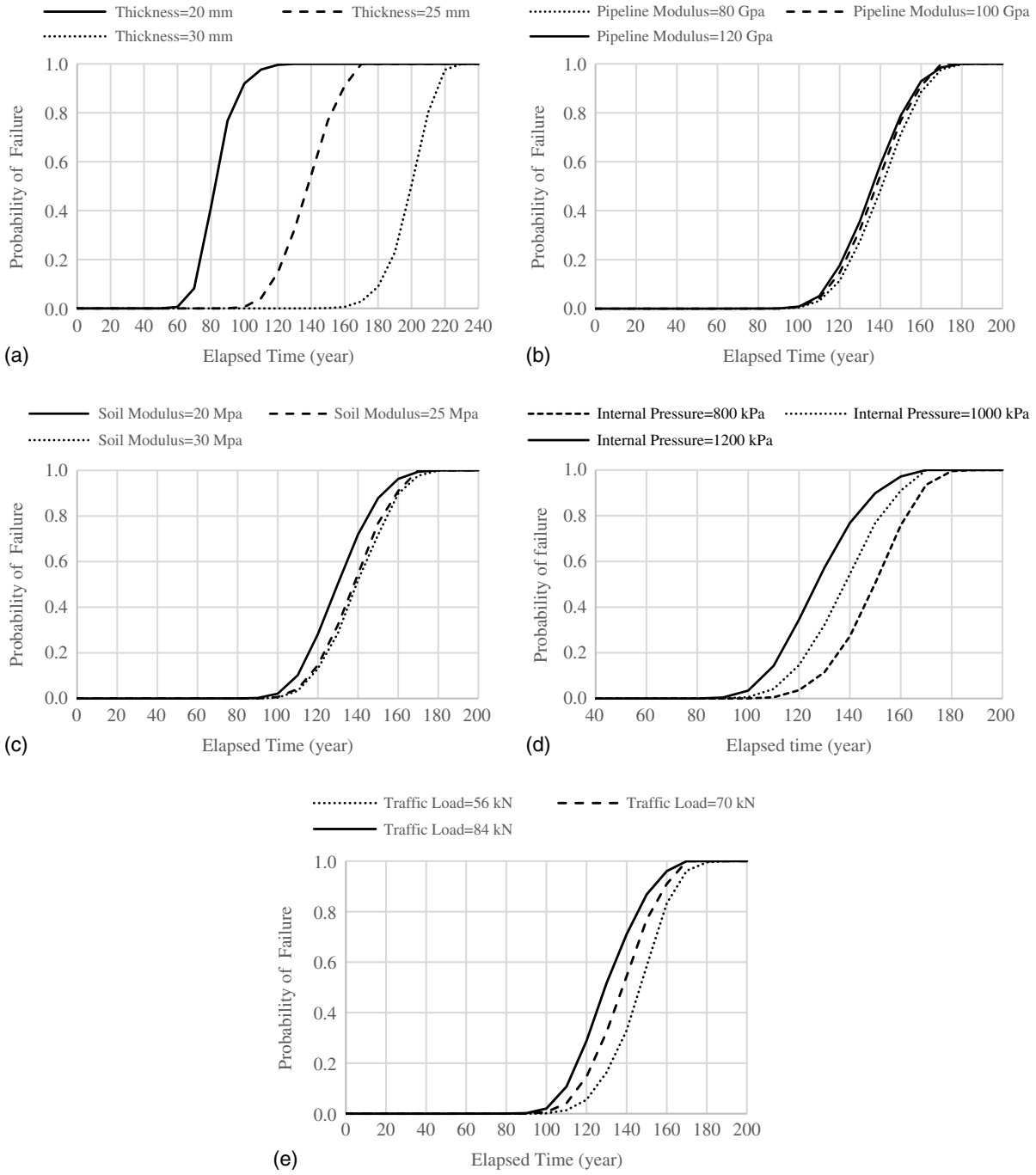

Fig. 7. Sensitivity analysis outcomes: variation in time-dependent failure probability curves due to the effect on failure probability of (a) thickness; (b) elastic modulus of pipe; (c) elastic modulus of soil; (d) internal pressure; and (e) traffic load.

pressure increased for aging pipelines. For example, the failure probability of a pipeline under 2 MPa pressure increased from 0 for a new pipeline to 0.28 at 90 years and 0.95 at 120 years, respectively.

Network Reliability Analysis

The reliability of a water distribution network refers to its ability to deliver a sufficient amount of water to communities. The network reliability can be categorized into two types: connectivity-based reliability, and hydraulic-based reliability. Connectivity-based reliability refers to the probability that the network remains physically connected (Yannopoulos and Spiliotis 2013). Hydraulic-based reliability, however, refers to the probability that all nodes are supplied with sufficient water quantities and pressure (Mazumder et al. 2019; Yannopoulos and Spiliotis 2013). This paper considered only the connectivity-based network reliability. Traditionally, there are three types of network reliability: source-sink reliability, *k*-out-of-*n* reliability, and all-terminal reliability. The 2-out-of-*n* reliability also is called source-sink reliability because it considers only the connectivity between the two nodes. The *k*-out-of-*n* reliability also allows some nodes to be isolated from the network. All-terminal reliability refers to the probability that all demand nodes are able to communicate with each other. This study applied

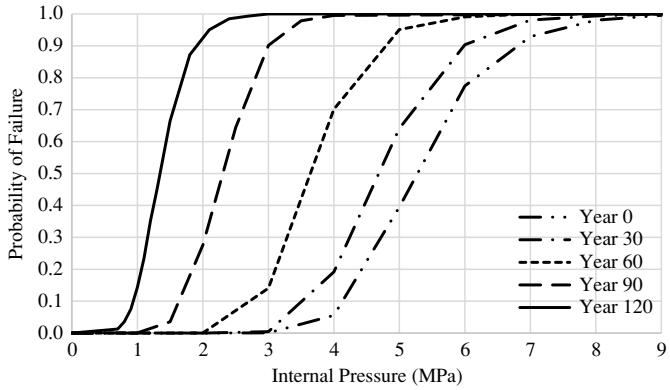

Fig. 8. Influence of internal pressure on fragility curves.

all-terminal reliability because all nodes in the network were required to have a water source. There are no perfectly reliable networks because unforeseeable events may cause interruption of the networks. When designing a water distribution network, the network needs to maintain operational status, so every node is connected to at least one source node. Thus, even if some pipes fail, access to water need to be maintained. In the present study, MCS and the graph decomposition method were used to determine the reliability of WDN.

Minimum Cut Set

In a graph network, a cut set can be referred to as a minimum cut set if the network fails when all pipelines in the cut set fail. The number of MCS in a network largely depends on the complexity and size of the network. For small networks, the MCS can be enumerated quickly by visual inspection. For complicated or large networks, however, an adjacency matrix is utilized to find the MCS (Chaturvedi 2016). The pipelines in the network are assumed to be statistically independent; in other words, the failure of one component does not affect the working condition of other pipelines. The failure probability of a minimum cut set can be determined as follows (Shinstine et al. 2002):

$$P(\text{MCS}_i) = \prod_{l=1}^{n_p} P_l \tag{12}$$

where $P(\text{MCS}_i)$ = failure probability of ith MCS that contains n_p number of pipelines; and P_l = failure probability of pipeline l.

It is assumed that the failure probability of MCS are statistically independent; hence, the network failure probability can be estimated as (Yannopoulos and Spiliotis 2013)

$$P_s = \sum_{i=1}^{M} P(\text{MCS}_i) \tag{13}$$

where M = number of significant MCS in network. The network reliability is the complement of its failure probability

$$R_s = 1 - P_s \tag{14}$$

Graph Decomposition

The graph decomposition model is used to simplify the network. This approach originally was proposed by Deuerlein (2008). The purpose of the decomposition is to provide efficient methods to operate and control large and complex networks. In the approach, all graph links are classified into one-connected links and biconnected block links. The degree of a node is defined as the number of components met at the node. Biconnected blocks are looped components whose nodes have degrees greater than or equal to 2. One-connected links are composed of forest links and bridge links (Deuerlein 2008). Bridge links are the components that connect biconnected blocks. The nodes with Degree 1 are marked as forest nodes, and forest links are the components that contain these nodes. The current forest links are removed from the network, and then the remaining network is checked for new forest links. This process is repeated until no more forest links can be found (Deuerlein 2008; Deuerlein et al. 2009).

The graph decomposition approach greatly helps network reliability calculation because it is a powerful tool to identify and simplify complex networks. Every biconnected block is represented by a block node, and thus a complex graph is simplified into a block graph. The reliability of each block node is computed separately, and then the network reliability can be calculated by theoretical probability equations on basis of graph layout. The all-terminal reliability of each block node and the block graph can be calculated as follows (Ramesh et al. 1987):

$$R_S = \sum_{i=0}^{n} M_i (1-b)^{m-i} b^i \tag{15}$$

where M_i = number of connected subgraphs with $(m-i)$ links, where m = number of total links and i = number of failure links; and b = failure probability of links.

An example WDN was used to illustrate and compare the network reliability obtained using MCS and graph decomposition technique. Fig. 9 shows the example network and the reliability blocks developed for the graph decomposition method. This network consisted of a reservoir, 27 nodes, and 34 pipelines. The numbers at the edge of the graph provide the pipeline identify number. The pipeline properties and loading conditions in this network were assumed to be the same as in the FEA models. Hence, the failure probability of pipelines determined in the fragility section was utilized to determine the reliability of the WDN. The number of MCS obtained utilizing the adjacent matrix method was described in detail by Yannopoulos and Spiliotis (2013). In this network, a total 46 MCS were found, including 10 1-pipeline MCS, 32 2-pipelines MCS, and 4 3-pipelines MCS. The number of pipelines in a MCS was considered up to three because no MCS contained four or more pipes. Fig. 9(b) shows the reliability block of the WDN. Deuerlein (2008) defined block nodes as biconnected blocks without forest links when key parts of the network are major concerns. The block nodes in this study, however, included the connected forest links because the reliability was calculated for the integrated network. The reliability of each block node was calculated first, and then the reliability of the block graph was estimated using the product of the reliabilities of block nodes.

Fig. 10 shows the network reliability calculated by the two methods. Corrosion had significant impacts on the network reliability because it quickly increased the failure probability of individual pipelines after a certain age. The two curves had similar trends up to 110 years, beyond which the MCS had lower values of network reliability. From the curve generated by the MCS, the network reliability decreased from 100% at 80 years to 52.71% at 110 years. From the curve generated by the graph decomposition method, the network reliability decreased from 100% at 80 years to 61.97% at 110 years.

If all the forest links are removed from a network, the remaining graph, containing biconnected blocks and bridge links, is called a two-core subgraph of the network. To generate a two-core

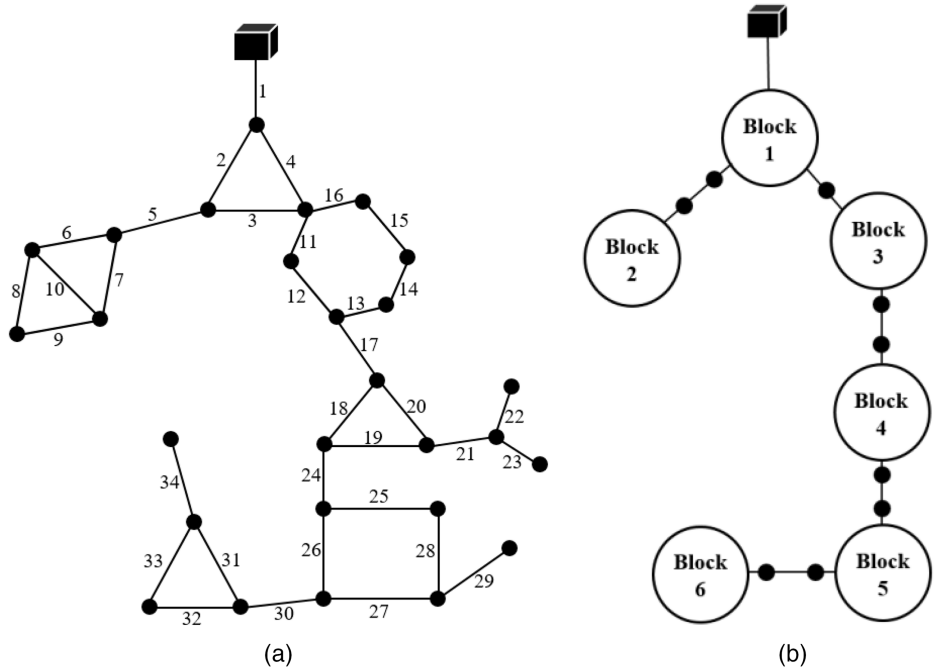

Fig. 9. (a) Example network graph; and (b) reliability block diagram.

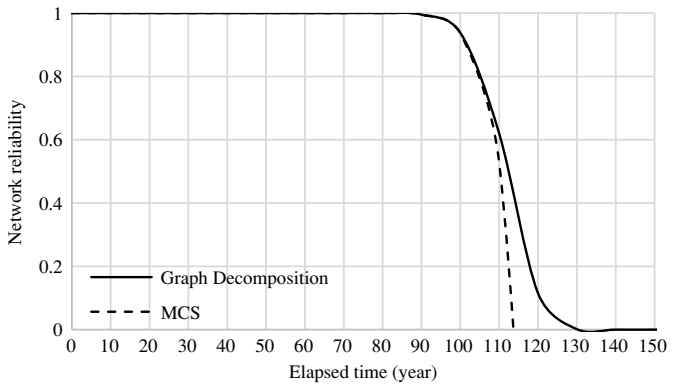

Fig. 10. System reliability of WDN.

subgraph, the pipelines at the ends of the network were removed (Fig. 11). For example, Pipes 21, 22, 23, 29, and 34 were removed. The reliability of the two-core network was calculated by the MCS and graph decomposition method. Fig. 12 shows the two-core network reliability curves calculated by two different methods. The results in Fig. 12 are similar to those in Fig. 10. The two-core network reliability was 100% at the beginning, and then it decreased quickly after passing 100 years. The MCS method provided lower reliability values than the graph decomposition method. Because two methods provided close network reliability values, the two methods are validated by each other up to 110 years. This is because the depth of the corrosion pit approaches the original thickness of the pipelines after about 110 years. Because the graph decomposition method simplifies the network graph, a difference was observed between the two approaches after 110 years of

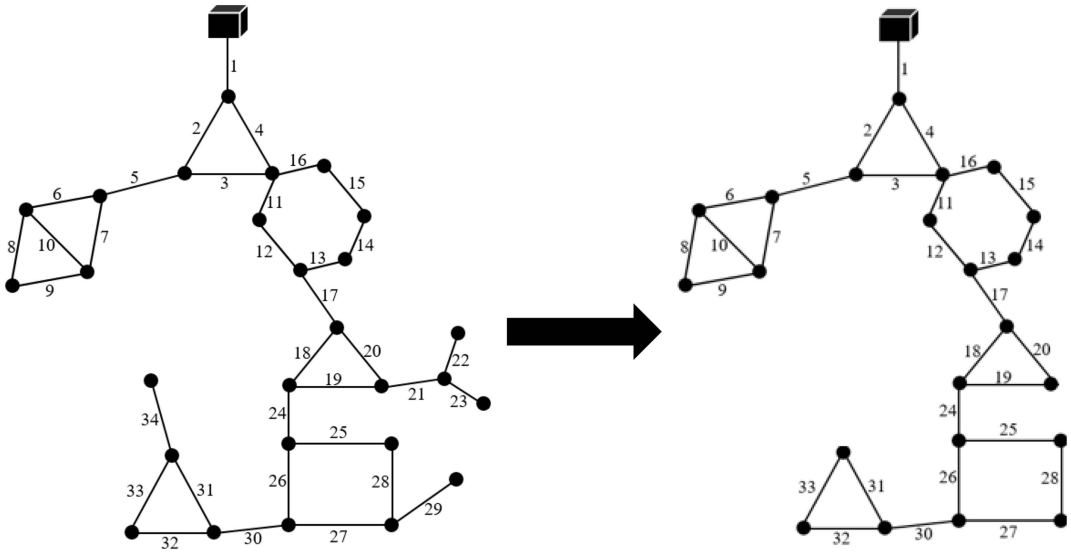

Fig. 11. Two-core subgraph of the example network.

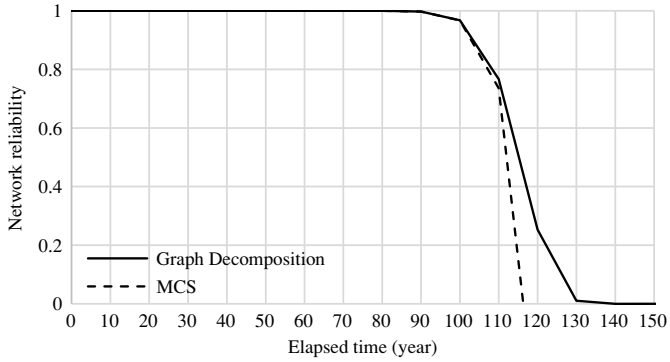

Fig. 12. Two-core network reliability curves.

pipeline age. It can be concluded that both methods are efficient ways to calculate network reliability because they are accurate, effortless, and convenient to use. The MCS method provides relatively lower reliability values because its reliability calculation depends largely on one-pipeline cut sets, and thus the network reliability decreases quickly as the failure probability of a single pipeline increases.

Conclusion

This study used FEA to generate fragility curves of buried water pipelines. After the FEA model was validated with the existing literature, the parameters were altered. The magnitude of circumferential stress was found to be the greatest of three types of stress; therefore, the failure probability of a pipeline was determined by comparing the circumferential stress on the pipeline with ultimate tensile strength of pipe material. To model uncertainties in geometries and loading cases, five parameters of the pipelines were varied to generate 243 analyses. The circumferential stresses obtained from the FEAs were fitted to a normal distribution. The burst failure probability of the pipeline then was estimated in a probabilistic manner using Monte Carlo simulation.

Fragility curves of the pipelines with exposure time were developed following three methods. The fragility curves developed by elastic ring theory and the modified Spangler formula had similar trends. The time-dependent failure probability curves developed utilizing the present FEA model provided better predictions than did the other two approaches. For example, stresses estimated for the example cast iron pipeline (diameter = 600 mm, and thickness = 25 mm) at 120 years were 83.05, 140.17, and 131.40 MPa using the present FEA, elastic ring theory, and the modified Spangler formula, respectively. The results obtained from the present approach were validated with recent study outcomes. Moreover, this paper investigated the relative importance of five parameters: pipe thickness, pipe elastic modulus, soil elastic modulus, internal pressure, and surface traffic load. It was found that the pipe thickness had the greatest impact on the failure probability, followed by internal pressure and surface traffic load. Aging pipelines are very sensitive to internal pressure, and the likelihood of failure probability increases with the ages.

This paper also compared the reliability of a WDN utilizing MCS and the graph decomposition method. An example WDN was analyzed to illustrate comparing the reliabilities estimated using the two approaches. The two reliability methods provided similar outcomes for the WDN, therefore they are verified by each other. The MCS provided relatively lower values of network reliability than did the graph decomposition approach. For example, network reliabilities at 110 years were 61.97% and 52.71% as estimated by network decomposition and MCS methods, respectively.

This study has a few limitations that need to be addressed in future research. This study was applied to large-diameter pipelines only. Further investigation is required for small-diameter pipelines. The reliability of the pipelines was determined by accounting for the effect of corrosion pit formation on the pipe wall. However, the influence of uniform corrosion was ignored. The joint effect of uniform and pitting corrosion on pipeline performance should be addressed in a future study. Additionally, uncertainties involved in corrosion growth were not considered. This study selected five factors for sensitivity analysis; other factors (e.g., buried depth) may need to be considered in the future.

Data Availability Statement

All data, models, and code generated or used during the study appear in the published paper.

Acknowledgments

The research described in this paper was supported in part by the National Science Foundation (NSF) Critical Resilient Interdependent Infrastructure Systems and Processes (CRISP) under Grant No. NSF-1638320. This support is gratefully acknowledged. However, the writers take sole responsibility for the views expressed in this paper, which may not represent the position of the NSF or their respective institutions.

Notation

The following symbols are used in this paper:

b = failure probability of pipe;
C = depth of soil cover (mm);
c_s = interception of bi-linear corrosion model (mm);
D = pipeline diameter (mm);
d = distance from pipeline to line of traffic load (mm);
E = elastic modulus of pipeline (GPa);
E' = elastic modulus of soil (MPa);
F_s = concentrated traffic load (kN);
h = burial depth (m);
I = moment of inertia of pipeline (mm^4);
i = number of link (pipeline) failures;
K = bending constant;
K_b = bending moment parameter;
K_Z = deflection parameter;
L_Δ = deflection lag factor;
m = number of total links;
N = number of Monte Carlo simulation;
n = number of failure simulations;
n_p = number of pipelines in ith MCS;
P_f = failure probability of pipeline;
P_l = failure probability of pipeline l;
P_s = failure probability network;
$P(\mathrm{MCS}_i)$ = probability of failure of ith MCS;
q = uniform vertical traffic load (kPa);
R = reliability of pipeline;

R_s = reliability of network;
r = radius of pipeline (mm);
T = exposure time (year);
T_1 = time after corrosion reaches steady state (year);
t = pipeline thickness (mm);
W = traffic load (kN);
W_{vertical} = vertical load due to soil cover and traffic load;
Z = limit state function
α and β = model coefficients;
ΔX = pipeline horizontal deflection (mm);
δ_s = rate of corrosion at steady state (mm/year);
κ = uncertainty coefficient;
ρ = internal pressure (kPa);
ρ_p = pressure transmitted to pipeline (kPa);
σ = stress on pipeline (MPa);
σ_a = resistance stress of pipeline (MPa);
σ_e = von Mises stress (MPa);
σ_s = maximum stress on pipe due to applied load (MPa);
σ_x = normal stress on pipe in x-direction (MPa);
σ_y = normal stress on pipe in y-direction (MPa);
σ_z = normal stress on pipe in z-direction (MPa); and
$\tau(T)$ = depth of corrosion (mm).

References

Ahammed, M. 1998. "Probabilistic estimation of remaining life of a pipeline in the presence of active corrosion defects." *Int. J. Press. Vessels Pip.* 75 (4): 321–329. https://doi.org/10.1016/S0308-0161(98)00006-4.

Ang, A. H. S., and W. H. Tang. 2007. *Probability concepts in engineering planning and design: Emphasis on application to civil and environmental engineering*. New York: Wiley.

Caleyo, F., J. L. Gonzalez, and J. M. Hallen. 2002. "A study on the reliability assessment methodology for pipelines with active corrosion defects." *Int. J. Press. Vessels Pip.* 79 (1): 77–86. https://doi.org/10.1016/S0308-0161(01)00124-7.

Caleyo, F., J. C. Velázquez, A. Valor, and J. M. Hallen. 2009. "Probability distribution of pitting corrosion depth and rate in underground pipelines: A Monte Carlo study." *Corros. Sci.* 51 (9): 1925–1934. https://doi.org/10.1016/j.corsci.2009.05.019.

Cerit, M., K. Genel, and S. Eksi. 2009. "Numerical investigation on stress concentration of corrosion pit." *Eng. Fail. Anal.* 16 (7): 2467–2472. https://doi.org/10.1016/j.engfailanal.2009.04.004.

Chaturvedi, S. K. 2016. *Network reliability: Measures and evaluation*. New York: Wiley.

De Leon, D., and O. F. Macías. 2005. "Effect of spatial correlation on the failure probability of pipelines under corrosion." *Int. J. Press. Vessels Pip.* 82 (2): 123–128. https://doi.org/10.1016/j.ijpvp.2004.07.018.

Deuerlein, J., A. Wolters, D. Roetsch, and A. R. Simpson. 2009. "Reliability analysis of water distribution systems using graph decomposition." In *Proc., World Environmental and Water Resources Congress 2009: Great Rivers*, 1–11. Reston, VA: ASCE.

Deuerlein, J. W. 2008. "Decomposition model of a general water supply network graph." *J. Hydraul. Eng.* 134 (6): 822–832. https://doi.org/10.1061/(ASCE)0733-9429(2008)134:6(822).

Folkman, S. 2018. *Water main break rates in the USA and Canada: A comprehensive study*. Logan, UT: Utah State Univ.

Ji, J., D. J. Robert, C. Zhang, D. Zhang, and J. Kodikara. 2017. "Probabilistic physical modelling of corroded cast iron pipes for lifetime prediction." *Struct. Saf.* 64 (Jan): 62–75. https://doi.org/10.1016/j.strusafe.2016.09.004.

Kucera, V., and E. Mattsson. 1987. *Corrosion mechanisms*. New York: M. Dekker.

Ling, Y. 1996. "Uniaxial true stress-strain after necking." *AMP J. Technol.* 5 (1): 37–48.

Masada, T. 2000. "Modified Iowa formula for vertical deflection of buried flexible pipe." *J. Transp. Eng.* 126 (5): 440–446. https://doi.org/10.1061/(ASCE)0733-947X(2000)126:5(440).

Mazumder, R. K., A. M. Salman, Y. Li, and X. Yu. 2018. "Performance evaluation of water distribution systems and asset management." *J. Infrastruct. Syst.* 24 (3): 03118001. https://doi.org/10.1061/(ASCE)IS.1943-555X.0000426.

Mazumder, R. K., A. M. Salman, Y. Li, and X. Yu. 2019. "Reliability analysis of water distribution systems using physical probabilistic pipe failure method." *J. Water Resour. Plann. Manage.* 145 (2): 04018097. https://doi.org/10.1061/(ASCE)WR.1943-5452.0001034.

Moser, A. P., and S. Folkman. 2008. *Buried pipe design*. 3rd ed. New York: McGraw-Hill.

Neya, B. N., M. A. Ardeshir, A. A. Delavar, and M. Z. R. Bakhsh. 2017. "Three-dimensional analysis of buried steel pipes under moving loads." *Open J. Geol.* 7 (1): 1. https://doi.org/10.4236/ojg.2017.71001.

Ostfeld, A. 2004. "Reliability analysis of water distribution systems." *J. Hydroinf.* 6 (4): 281–294. https://doi.org/10.2166/hydro.2004.0021.

Petersen, R. B., and R. E. Melchers. 2012. "Long-term corrosion of cast iron cement lined pipes." In *Proc., Corrosion and Prevention 2012*. Melbourne, Australia: Australasian Corrosion Association.

Petersen, R. B., and R. E. Melchers. 2014. "Long term corrosion of buried cast iron pipes in native soils." In *Proc., ACA Conf., Darwin*, 21–24. Melbourne, Australia: Australasian Corrosion Association.

Qian, G., M. Niffenegger, D. R. Karanki, and S. Li. 2013a. "Probabilistic leak-before-break analysis with correlated input parameters." *Nucl. Eng. Des.* 254 (1): 266–271. https://doi.org/10.1016/j.nucengdes.2012.10.005.

Qian, G., M. Niffenegger, W. Zhou, and S. Li. 2013b. "Effect of correlated input parameters on the failure probability of pipelines with corrosion defects by using FITNET FFS procedure." *Int. J. Press. Vessels Pip.* 105 (May): 19–27. https://doi.org/10.1016/j.ijpvp.2013.02.004.

Rajani, B., and J. Makar. 2000. "A methodology to estimate remaining service life of grey cast iron water mains." *Can. J. Civ. Eng.* 27 (6): 1259–1272. https://doi.org/10.1139/l00-073.

Ramesh, A., M. O. Ball, and C. J. Colbourn. 1987. "Bounds for all-terminal reliability in planar networks." *Anal. Discrete Math.* 144: 261–273. https://doi.org/10.1016/S0304-0208(08)73060-3.

Robert, D. J., P. Rajeev, J. Kodikara, and B. Rajani. 2016. "Equation to predict maximum pipe stress incorporating internal and external loadings on buried pipes." *Can. Geotech. J.* 53 (8): 1315–1331. https://doi.org/10.1139/cgj-2015-0500.

Shinstine, D. S., I. Ahmed, and K. E. Lansey. 2002. "Reliability/availability analysis of municipal water distribution networks: Case studies." *J. Water Resour. Plann. Manage.* 128 (2): 140–151. https://doi.org/10.1061/(ASCE)0733-9496(2002)128:2(140).

Spangler, M. G. 1941. *The structural design of flexible pipe culverts*. Ames, IA: Iowa State College of Agriculture and Mechanic Arts.

Tung, Y. K. 1985. "Evaluation of water distribution network reliability." In *Unknown host publication title*, 359–364. Reston, VA: ASCE.

Wang, N., and M. S. Zarghamee. 2014. "Evaluating fitness-for-service of corroded metal pipelines: Structural reliability bases." *J. Pipeline Syst. Eng. Pract.* 5 (1): 04013012. https://doi.org/10.1061/(ASCE)PS.1949-1204.0000148.

Wang, W., A. Zhou, G. Fu, C.-Q. Li, D. Robert, and M. Mahmoodian. 2017. "Evaluation of stress intensity factor for cast iron pipes with sharp corrosion pits." *Eng. Fail. Anal.* 81 (3): 254–269. https://doi.org/10.1016/j.engfailanal.2017.06.026.

Warman, D. J., J. D. Hart, and R. B. Francini. 2009. *Development of a pipeline surface loading screening process & assessment of surface load dispersing methods*. Worthington, OH: Canadian Energy Pipeline Association.

Watkins, R. K., and L. R. Anderson. 1999. *Structural mechanics of buried pipes*. London: CRC Press.

Yannopoulos, S., and M. Spiliotis. 2013. "Water distribution system reliability based on minimum cut–set approach and the hydraulic availability." *Water Resour. Manage.* 27 (6): 1821–1836. https://doi.org/10.1007/s11269-012-0163-5.

Zhang, J., Z. Liang, and G. Zhao. 2016. "Mechanical behaviour analysis of a buried steel pipeline underground overload." *Eng. Fail. Anal.* 63 (Jan): 131–145. https://doi.org/10.1016/j.engfailanal.2016.02.008.

Zhang, P., L. Su, G. Qin, X. Kong, and Y. Peng. 2019. "Failure probability of corroded pipeline considering the correlation of random variables." *Eng. Fail. Anal.* 99 (Sep): 34–45. https://doi.org/10.1016/j.engfailanal.2019.02.002.